Effect of Axisymmetric Magnetic Field Strength on Heat Transfer from a Current-Carrying Micro-Wire in Ferrofluid

Vinay Kumar[1,2*], Mario Casel[1], Van Dau[1,3], Peter Woodfield[1]

[1]School of Engineering, Griffith University, Gold Coast, QLD 4222, Australia

[2]Queensland Micro and Nanotechnology Centre, Brisbane, QLD 4111, Australia

[3]Centre for Clean Environment and Energy, Griffith University, Gold Coast, QLD 4222, Australia

Corresponding Author*-vinay.kumar@griffithuni.edu.au

Abstract

The effect of the strength of the self-induced magnetic field around a current carrying wire on thermomagnetic convection cooling in ferrofluid is experimentally and numerically investigated. Temperature-rise characteristics of the hot micro-wire for uniform Joule heating with different electric currents are compared to identify the relative importance of the strength of the axisymmetric magnetic field. Experiments are done with copper and platinum wires with current inputs adjusted to achieve the same Joule heating per unit length of wire. It was found that at high current supply (2A), mixing in ferrofluid is escalated due to thermomagnetic convection that resulted into 28 % increase in average Nusselt number value which finally resulted into temperature drop of 8 K in comparison to DIW. Comparison of results for different self-induced magnetic field strengths in ferrofluid and deionized water clearly show that the observed cooling phenomenon is due to the self-induced magnetic field interacting with the magnetic fluid rather than natural-convection or other nanofluid-related mechanisms. For 1.83 W Joule heating, the temperature of the copper wire is 6 K lower than that of the platinum wire. Temperature and velocity contours obtained from simulations based on a 2-D single-phase model including a temperature-dependent magnetic body force provide flow visualization and further confirmed that the thermomagnetic cooling is responsible for the observed behaviour.

Keywords: Joule-Heating; Self-induced Magnetic Field; Ferrofluid; Heat Transfer; Thermomagnetic Convection; Cooling.

Nomenclature

Notations		***Subscripts***	
$\bar{h}$	Average heat transfer coefficient, $\frac{W}{m^2K}$	m	Magnetic
Ra	Rayleigh number	b	Buoyancy
f	Body force	eff	Effective
c	Specific Heat, $\frac{J}{kgK}$	p	Particle
k	Thermal conductivity, $\frac{W}{mK}$	f	Base fluid
I	Electric current, A	fr	Freezing
$\vec{B}$	Magnetic Field, $\frac{Nm}{A}$	0	Reference value
$\vec{H}$	Magnetic field strength, $\frac{A}{m}$	r	Radial component
$\vec{M}$	Magnetization, $\frac{A}{m}$	s	Saturation
r	Radius, m	***Greek symbols***	
Re	Reynolds Number	$\boldsymbol{\mu_0}$	Vaccum magnetic permeability; $4\pi \times 10^{-7}\ \frac{N}{A^2}$
Pr	Prandtl Number	$\boldsymbol{\chi}$	Magnetic susceptibility
T	Temperature (K)	$\boldsymbol{\epsilon}$	Particle concentration
$\overline{Nu}$	Nusselt Number	α	Temperature coefficient of Electric Resistance, $\frac{1}{K}$
d	Diameter of wire; m	μ	Dynamic viscosity; $\frac{kg}{ms}$
k_b	Boltzmann Constant; $1.3806 \times 10^{-23}\ \frac{J}{K}$	ρ	Density; $\frac{kg}{m^3}$
u_B	Brownian mean Velocity	γ	Thermal expansion coefficient of ferrofluid; K^{-1}
R_a	Gravity Rayleigh Number	a	Thermal Diffusivity of Ferrofluid; $\frac{m^2}{s}$

R_{am}	Magnetic Rayleigh Number	L	Characteristic Length; m
R	Resistance; Ω	***Abbreviations***	
q_s	Surface Heat flux; $\frac{W}{m^2}$	AC	Alternating Current
C	Curie Constant; $8\times10^{-7}\,K^{-2}$	DC	Direct Current
G_r	Grashof Number; $\frac{g\beta(T-T_0)L^3}{\upsilon^2}$		

1. Introduction

Ferrofluid consists of a stable dispersion of single-domain superparamagnetic nanoparticles in a non-magnetic base- fluid (commonly water, oil and kerosene). It is a unique class of nanofluid that exhibits both fluidity like Newtonian fluids and magnetic properties like ferro-magnetic materials. Addition of ferroparticles in the base-fluid upgrades the thermo-physical, rheological and thermal characteristics and these properties are affected by the strength and orientation of the applied magnetic field **[1-2]**. This actuating behaviour enables to control the particles' movement, fluid flow and cooling which make the ferrofluid a promising media for space applications (propulsion medium), biomedical engineering, industrial heat exchangers, electronic packaging and energy harvesters **[3]**.

In the last decade, ferrofluids have attracted the attention of many researchers for heat transfer and cooling applications **[4-7]**. Ferrofluids have a property that as the temperature becomes lower, Brownian motion is weaker and the superparamagnetic nanoparticles in the liquid align more easily with the magnetic field (i.e. the magnetic susceptibility increases with reducing temperature). As a result of this, a phenomenon called thermomagnetic convection can occur in ferrofluids if there is a temperature gradient present **[8]**. Thermal expansion of the fluid leading to fewer particles per unit volume in hot regions is another mechanism for the variation in magnetic properties with temperature **[9]**. The phenomenon is analogous to natural convection driven by the buoyancy effect.

In recent years, a large proportion of the literature on this heat transfer phenomenon has focused on externally applied magnetic fields which may be constant or varying in time and space. Shuchia et al. **[11]** reported the effect of an external magnetic field around hot spots on heat

transfer enhancement using ferrofluid. Goharkhah et al. **[12]** studied forced convection and pressure drop characteristics in ferrofluid under the influence of uniform and alternating magnetic fields. They reported a 16.4% heat transfer enhancement in ferrofluid in comparison to de-ionized water. With application of alternating and uniform magnetic fields, the heat transfer rate was intensified by 37.3% and 24.8%, respectively. Mehrali et al. **[13]** analysed the local heat transfer coefficient and thermal efficiency index as function of fluid velocity for hybrid graphene-based ferrofluid and found that the local convective heat transfer coefficient increased by 4% in the presence of the magnetic field. Some further recent experimental studies on heat transfer intensification in ferrofluids are listed in **Table 1**. Almost all studies considered report heat transfer enhancements with an exception being a boiling heat transfer study in ferrofluid by Vatani et al. **[14]**.

Table 1: Representative recent experimental studies on thermomagnetic convection

Geometry	**Magnetic Field**	**Key Findings**	**Ref.**
Rectangular cell	Uniform field using electromagnet	Heat transfer augmentation with magnetic field.	Wen and Su **[18]**
Horizontal cell	Helmholtz coil (uniform field)	Magneto-viscous effect has a stabilizing effect on thermomagnetic convection.	Enger et al. **[10]**
Rectangular cell	Non-uniform magnetic field using permanent magnets	Higher heat transfer enhancement than natural thermo-gravitational convection.	Zablotsky et al. **[19]**
Heated tube	Uniform magnetic field	Increase in h is proportional to applied magnetic field and concentration of ferroparticles.	Lajvardi et al. **[20]**
Heated wire	Self-induced magnetic field	More effective cooling and diminished delay to onset of convection compared with natural convection.	Vatani et al. **[17]**

Heated wire	Self-induced magnetic field	Suppression of heat transfer under boiling conditions	Vatani et al. **[14]**

In relation to practical devices, ferrofluids have great potential for heat transfer enhancement at small scales. In miniaturized thermal systems, heat transfer is limited by diffusion due to flow limitations. Enhancing and controlling the convection in these systems using ferrofluids can be a method of overcoming this barrier. Xuan et al. **[15]** fabricated a device to generate thermomagnetic convection loop for cooling of a chip. The setup used the magnet and waste heat from chip to maintain the flow of ferrofluid to dissipate the heat. With a magnetic field, higher cooling was reported due to enhanced thermomagnetic convection. Krauzina et al. **[16]** analysed the convection phenomenon in ferrofluid having transformer oil as the carrier fluid. The ferrofluid was inserted in a spherical cavity under a co-axial magnetic field. When the cavity was heated from the top, the Nusselt number increased and by heating from bottom, the Nusselt number decreased with magnetic intensity. In the latter case, it was proposed that the increase in the concentration of particles raises the viscosity and obstructs the development of natural convection.

Numerical studies provide valuable insight into flow behaviour and the underlying mechanisms of thermomagnetic convection. Moreover, it is possible to explore the effects of geometrical arrangements in relation to heat transfer enhancement for thermal engineering design. **Table 2** lists some recent numerical studies that have been conducted to analyse the fluid flow and heat transfer enhancement by ferrofluids in different geometries including rectangular, cylindrical, ribbed microchannels and porous cavities. In most of the studies, laminar flow is simulated and effects of magnetic field intensity, magnetic field orientation, ferroparticle concentration, Reynolds number and type of magnetic field (uniform or non-uniform) have been investigated.

Given that there are variations in the formulation of the underlying theory of thermomagnetic convection (e.g. two-phase and single-phase models in **Table 2**), it is important to experimentally verify the results of numerical simulations. Unfortunately, as it is also shown in **Table 2**, many numerical studies did not include comparisons with experiment. This highlights the fact that there is currently a lack of sufficiently detailed experimental data on thermomagnetic convection available in the literature for this purpose. Also as indicated by

comparing **Tables 1** and **2**, in general, the number of experimental studies on thermomagnetic convection in the literature is significantly lower than the number of numerical studies.

This study aims to provide a more rigorous set of experimental data than has been available to date for thermomagnetic convection around a current carrying microwire in ferrofluid. Moreover, to the knowledge of the authors, no studies on thermomagnetic convection have considered magnetic field strength from a current-carrying wire independently of the heat flux boundary condition. In this work, this is achieved using wires of two different materials – copper and platinum. The electric current is adjusted to maintain the same Joule heating for both materials. Thus, the thermal boundary condition and geometry can be identical for both cases, but a significantly larger current is required for the copper wire due to the lower electrical resistance. The increased current means a stronger magnetic field is present. A numerical model for thermomagnetic convection is presented and tested against the collected data. The major contributions of this present study are as follows;

- Identify the relative effect of thermomagnetic convection in comparison to natural convection for cooling of micro-wires.
- Effect of self-induced non uniform magnetic field on thermomagnetic convection phenomenon at same boundary conditions.
- Identification of hotspots around wire during thermomagnetic convection
- Velocity and temperature distribution in fluid domain for a better understanding and visualization of the flow at higher current supply and notable timings.

Foregoing study targeting the understanding the heat sources, heat dissipation and improving the flow path for heat removal will be great potential benefit and will enhance the performance of miniaturised type heat transfer devices.

Table 2: Representative recent numerical studies on thermomagnetic convection

Geometry	**Simulation Method**	**Magnetic Field**	**Experimental Verification**	**Key Findings**	**Ref.**
Porous Cavity	Lattice Boltzman	Uniform magnetic field	No	Heat transfer capacity is proportional to magnetic field intensity.	Jin et al. **[21]**

2D enclosure	Single Phase Model	Magnetic field by dipole	No	The Nusselt number scales with $Ra_m^{0.25}$	Mukhopadyay et al. **[22]**
Cylinder	Two-phase model	Uniform magnetic field	No	Heat transfer coefficient is the function of magnetic strength, decreases with particle size.	Jafari et al. **[23]**
Square Cavity	Single Phase Model	Non-uniform magnetic field	No	Intensification of magnetic field increases the fluid flow and heat transfer.	Ashouri et al. **[24]**
Parallel plates	Single Phase Model	Non-uniform magnetic field	No	Thermal gradient caused inhomogeneous magnetic body force that inhibits convection.	Strek and Joseph **[25]**
Square Channel	Two-phase model	Uniform Magnetic field by permanent Magnets	No	Magnetic field induced mixing in flow and disturbance in boundary layer development.	Bahiraei et al. **[26]**
Cylindrical	Two-phase model	Self-induced non uniform field	Model validated with previous experimental results	Higher self-induced magnetic field creates disturbance in the thermal boundary layer that increases	Hangi et al**.** **[27]**

				the heat transfer rate.	
Heated wire	Single-phase model	Self-induced	Yes	Flow Circulation around wire depends upon applied current	Vatani et al. **[28]**
Cylindrical	Single-phase model	Uniform external magnetic field	No	Effect of conductor shape is critical for heat transfer enhancement	Krako and Nikiforov **[9]**
Square Cavity	Single-phase model	Non uniform external magnetic field	No	At high magnetic fields, thermomagnetic convection sets-in and makes gravitational effects relatively negligible.	Cunha et al. **[29]**
Square Enclosure	Single-phase model	Non uniform external magnetic field	No	Transition in convection is reported by the change in flow behaviour	Szabo and Früh **[30]**
Mini-channel	Single-phase model	Alternating magnetic field	No	Critical frequency is observed for heat transfer, diffusion in stagnant layers for AC supply	Singh et al**.** **[31]**

Circular Ring	Single-phase model	Non-uniform external magnetic field using permanent magnets	No	Effect of magnetic field and geometric design in flow characteristics of magnetic nanofluid	Dalvi et al. **[32]**
T-Junction	2-D single phase model	Non-uniform external magnetic field using mutli-wire system	Yes	200% increment in average local heat transfer, development of vortices in magnetic field, significant cooling effect	Gerdroodbary et al.**[33]**
Semi-annulus	2-D laminar model	Non-uniform external magnetic field	Yes	Change in viscosity with magnetic field, augment of Nusselt number with volume fraction	Sheikholeslami et al.**[34]**
Double-pipe cylinder	2-D laminar model	Non-uniform external magnetic field	Yes	Radiation heat transfer, Brownian motion analysis, Nusselt number augments with increase in Lorentz forces	Sheikholeslami et al.**[35]**

Horizontal parallel plates	Two-phase model	Combined effects of radiation and magnetic field	Yes	Boundary layer thickness decreases and Nusselt number increases with radiation intensity.	Sheikholeslami et al.**[36]**
Rotating double cylinder	Two-phase model	External magnetic field	Yes	Effect of Lorentz forces and Brownian motion on heat transfer characteristics of Al_2O_3-H_2O	Shafee et al.**[37]**

2. The Model

We analysed thermomagnetic convection around current carrying wire as presented in **Fig.1.** The wire is inserted in the channel and orientated vertically so the gravity force is parallel with the wire's direction (z-axis). The fluid under investigation is in a static condition in the channel and is exposed to the self-induced magnetic field generated by passing the electrical current through the wire. The temperature gradient and magnetic field can be expected to be axis-symmetric in every plane perpendicular to the z-axis. Hence the problem can be reduced to a 2-dimensional domain considering the fluid flow in vertical (z) and radial (r) directions. We may note from some studies such as **[9]** and **[38]** that three-dimensional effects are quite possible for this geometry with convection cells in the azimuthal direction. However, for the present purpose, the 2D model will suffice. As the channel is exposed to an isothermal bath, the boundary conditions for the whole domain are isothermal as shown in **Fig.1**. The initial condition is a uniform temperature and then an electric current is supplied to the wire providing both heating and a magnetic field to drive thermomagnetic convection. The transient temperature of the wire is the output from the model.

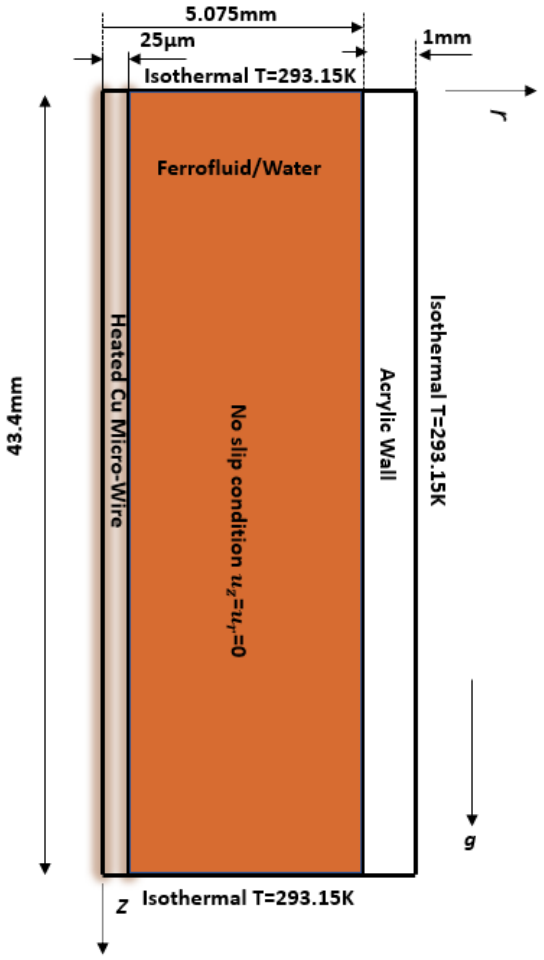

Fig.1: Two-dimensional axisymmetric model

3. Mathematical and Numerical Formulation

3.1 Governing Equations

A single-phase model with no slip conditions is used to simulate natural and thermomagnetic convection in ferrofluid around a vertical transient hot micro-wire. The convection phenomenon is governed by mass conservation, momentum and energy equations for a viscous and incompressible fluid, including natural convection. For thermomagnetic convection, the Curie law and Langevin magnetization law are used to describe the ferroparticle behaviour with temperature change occurring in fluid domain, leading to the thermomagnetic body force. Considering the above assumptions, the governing conservation equations are:

$$\nabla \cdot u = 0; \quad \textbf{(1)}$$

$$\rho\left(\frac{\partial u}{\partial t} + (u \cdot \nabla)u\right) = -\nabla p + \mu\Delta u + f_b + f_m; \quad \textbf{(2)}$$

$$\rho c_p\left(\frac{\partial T}{\partial t} + (u.\nabla)T\right) = \nabla.(k\nabla T) + \varphi; \quad \textbf{(3)}$$

where φ denotes the heat source due to Joule heating from the electrically heated wire and f_b and f_m represent the gravity-induced and thermomagnetic body force, respectively. The Joule

heating is caused by the voltage drop over the resistance and is described by Ohm's law as well as Joule's first law;

$$\varphi = J^2\beta(1 + \alpha\Delta T) \quad \textbf{(4)}$$

where J, β, α are the current density, temperature coefficient and electrical resistivity of the heated wire, respectively.

The first term is modelled by the Boussinesq approximation for temperature-driven buoyancy **[44]** and is assumed to only act in vertical direction due to the configuration's alignment with the gravity field. The radially directed thermomagnetic body force results from the interaction of ferromagnetic particles suspended in the fluid, interacting with the magnetic field induced by the current carrying wire **[43];**

$$f_{m,r} = \mu_0 M \frac{\partial}{\partial r}(M + H) \quad \textbf{(5)}$$

where μ_0 is the vacuum permeability, M and H are the magnitude of ferrofluid magnetization and the magnetic field strength. In case of electrically heated wire, both can be linked to the I by

$$H = \frac{I}{2\,\pi\, r}; \quad \textbf{(6)}$$

$$M = L(\xi)M_\infty \quad \textbf{(7)}$$

The RHS of **Eqn. (7)** describes the Langevin magnetization law **[45]** where M_∞ denotes the saturation magnetization of the fluid and where $L(\xi)$ is the Langevin function

$$L(\xi) = \coth(\xi) - \frac{1}{\xi} \approx \frac{\xi}{3} \quad \textbf{(8)}$$

which is approximated by a Taylor expansion up to the first order. The Langevin parameter ξ is;

$$\xi = \mu_0\, \pi \frac{M_S(T) d_p^3\, H}{6\, k_B\, T} \quad \textbf{(9)}$$

where M_s, d_p and k_B denote the saturation magnetization of the ferromagnetic particles, the particles' diameter and the Boltzmann constant, respectively. After applying the Curie-law for demagnetization, and additionally accounting for thermal expansion effects of the fluid phase the saturation magnetization terms M_s and M_∞ can be expressed in terms of temperature. Substituting **Eqs. (6,7,8 and 9)** into **(5),** finally, the thermomagnetic body force in radial direction yields

$$f_{m,r} = -\frac{\mu_0 I^2}{4\pi^2 r^3}(\chi_0 T_0 f(T) + 1)\chi_0 T_0\, f(T) \quad \textbf{(10)}$$

where the reference susceptibility at reference temperature T_0 identifies as

$$\chi_0 = M_{\infty,0}\, M_{s,0}\, \frac{\mu_0 \pi\, d_p^3}{18\, k_B T_0} \quad \textbf{(11)}$$

$M_{\infty,0}$ is the fluid's saturation magnetization, with a similar behaviour to the solid phase's magnetization change with temperature **[45]**

$$M_\infty = M_{\infty 0}\, \frac{1-CT^2}{1-CT_0^2}\, (1-\gamma(1-\epsilon)(T-T_0)) \quad (12)$$

γ is here the thermal expansion coefficient, where γ and C are the magnetic particles' volumetric concentration and the Curie constant respectively.

Considering the **Eqn.** (7) and the relation between Magnetization and magnetic field i.e. $M = \chi H$, the Langevin's magnetization law (**Eqn**. (11) yields.

$$\chi_L(T) = M_{\infty 0} M_{s0}\, \frac{\mu_0 \pi\, d_p^3}{18\, k_B} \left(\frac{1-CT^2}{1-CT_0^2}\right) \frac{(1-\gamma(1-\epsilon)(T-T_0))}{T} \quad (13)$$

And the initial susceptibility at the T_0 will be,

$$\chi_0 = \chi_L(T = T_0) = M_{\infty 0} M_{s0}\, \frac{\mu_0 \pi\, d_p^3}{18\, k_B T_0} \quad (14)$$

The initial susceptibility is given as χ_0 =1.88, the change with temperature can be expressed as

$$\chi_L(T) = \chi_0 T_0 f(T) \quad (15)$$

On comparing the **Eqs.** 13,14 and 15

$$f(T) = \left(\frac{1-CT^2}{1-CT_0^2}\right) \frac{(1-\gamma(1-\epsilon)(T-T_0))}{T} \quad \textbf{(16)}$$

where ϵ, γ and C are the ferroparticles volumetric concentration, thermal expansion coefficient and the Curie Constant respectively.

Buoyancy-induced flow effects are characterized by the gravity Rayleigh number (R_a) and magnetic Rayleigh number (R_{am}) for the cases of natural convection and thermomagnetic convection.

$$R_a = \frac{g\gamma(\mathrm{T}-T_0)L^3}{a.\mu_{eff}}; \quad (17)$$

Where γ, a and μ_{eff} is the thermal expansion coefficient, thermal diffusivity and dynamic viscosity of tested ferrofluid. Correspondingly,

Correspondingly, the value for R_{am} [**47**];

$$R_{am} = \left(1 + \frac{1}{\gamma T_0}\right)\left(\frac{g M_n \gamma(\mathrm{T}-T_0) d^3}{2\lambda \upsilon}\right); \quad (18)$$

$$d = \frac{6L}{\left(\frac{Gr}{4}\right)^{0.25}} \text{ and } Mn = \frac{\mu_0 H^2 L^2}{\rho \lambda} \quad (19)$$

Where d is the thickness of the boundary layer, M_n is the magnetization number and υ is the kinematic viscosity of ferrofluid. As both the gravity Rayleigh number (<10^4) and

thermomagnetic Rayleigh number (<10^7) are below the critical value for the onset of turbulence in the current analysis, the flow is considered as laminar.

3.2 Thermophysical Properties of Ferrofluid

Besides the thermomagnetic properties of ferrofluid, the nanoparticles suspended inside the base fluid result in a modification of the following properties relevant for the flow under investigation. The specific heat capacity and density of nanofluids are evaluated as;

$$c_{p,eff} = \frac{(1-\epsilon)\rho_f c_{p,f} + \epsilon \rho_p c_{p,p}}{\rho_{eff}} \quad \textbf{(20)}$$

$$\rho_{eff} = \epsilon \rho_p + (1-\epsilon)\rho_f \quad \textbf{(21)}$$

where subscripts $eff, f\ and\ p$ refers to nanofluid, base fluid and suspended particles properties **[46].** As a function of volume fraction (ϵ), the relations for effective thermal conductivity and effective dynamic viscosity **[39];**

$$k_{eff} = k_f\left(1 + 4.4Re^{0.4}Pr^{0.66}\left(\frac{T}{T_{fr}}\right)^{10}\left(\frac{k_p}{k_f}\right)^{0.03}\epsilon^{0.66}\right) \quad \textbf{(22)}$$

Where the nanoparticles Reynolds number is defined as;

$$Re = \frac{\rho_f \text{u}_B d_p}{\mu_f} \quad \textbf{(23)}$$

Eqn. (24) gives a relation between the particles dynamic velocity and their inertia, resulting from the Brownian mean velocity:

$$\text{u}_B = \frac{2k_b T}{\pi \mu_f d_p^2} \quad \textbf{(24)}$$

The effective dynamic viscosity of a nanofluid yields;

$$\mu_{eff} = \frac{\mu_f}{1-34.87\left(\frac{d_p}{d_f}\right)^{-0.3}\emptyset^{1.03}} = \frac{\mu_f}{0.883} \quad \textbf{(25)}$$

3.3 Numerical Implementation

The model was implemented with the commercial finite-volume method, Ansys FLUENT. An incompressible laminar flow solver using the SIMPLE algorithm was selected. A second-order upwind strategy was employed for the convection terms with a fully implicit time scheme for the unsteady terms. As the software does not support the ferrohydrodynamic problems, the magnetic body force term and ferrofluid properties described above were coded up in C-language and were compiled and linked to run as user-defined functions within the code. Non-uniform grid spacing was employed with the finest spacing in the vicinity of the wire surface. Grid dependence and time step dependence tests were carried out to establish a robust and

reliable numerical solution. Normalized residuals converged by several orders of magnitude each time step. **Fig. 2** illustrates that grid convergence is achieved with greater than 150 cells in the radial direction. The following refers to n_w and n_f, standing for the number of cells in radial direction for the wire and water domains.

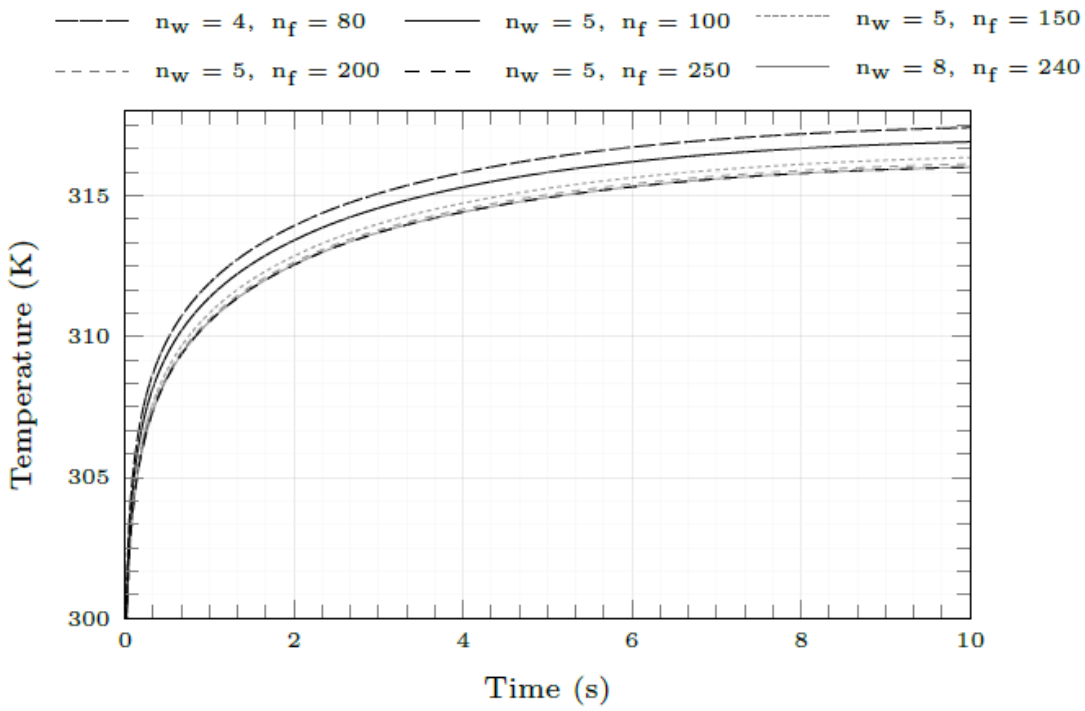

Fig. 2: Computational mesh sensitivity- Natural convection simulation for Cu wire at 1.5 A

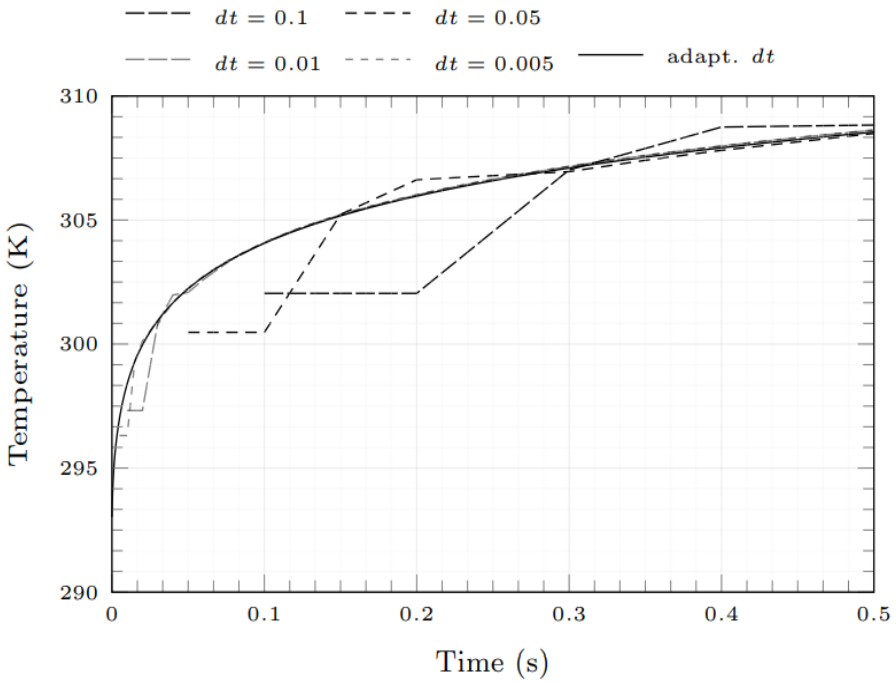

Fig. 3: Time step sensitivity- Natural convection simulation for Cu wire at 1.5 A

Fig. 3 shows the evolution of the average wire temperature in DIW using different time step sizes. It appears that the time step size has the largest impact on the resolution in the early stage of the simulation, whereas it converges for later points in time. As we intend to analyse all effects, including the temperature evolution at the beginning, a time step size of dt >0.005s is not acceptable in the early stage. Therefore, we decided for an adaptive time step scheme where the smallest step size is chosen as dt_min = 10^{-5}s. Such a scheme guarantees to capture the phenomenon all the time during simulation process.

4. Experimental Set-up and Measurement

Four identical transient hot wire measurement cells were developed to measure the temperature rise in the heated micro-wire with respect to time. Measurement cells are transparent square channels, 43.4 mm in length and 10.15×10.15 mm^2 cross-section, with either a 50-µm diameter copper or platinum micro-wire passing centrally through the measurement cells. A schematic diagram of the designed cell is shown in **Fig.4.** The cell is transparent to affirm that it is completely filled with ferrofluid from bottom to top, no bubbles are in the fluid due to the air in the cell and no build-up of ferroparticles on the micro-wire surface from previous experiments.

Experiments were conducted inside an Isotech^{TM} Europa 4520 temperature-controlled bath to ensure iso- thermal conditions of 293.15 K around the cell. A constant current was supplied (KEITHLEY 2200-20-5, US) to the microwire for 12 s to produce the axis-symmetric self-induced magnetic field and generate heat by Joule heating. The tested ferrofluid (EMG 807) is provided by FerrotecTM, is a dispersion of magnetite (Fe_3O_4) nanoparticles with a diameter of 10 nm and 2% volume concentration in de-ionized water. The properties of tested ferrofluid are presented in **Table 3.**

Components (% by Volume)			ρ_{eff}	μ_{eff}	χ_0	γ	$c_{p,eff}$	k_{eff}	a
Fe_3O_4 Particles	Surfactant	De-ionized water	1100 kg/m^3	4.5 mPa·s	1.88	7.7×10^{-4} K^{-1}	3.78 $\frac{kJ}{kgK}$	0.62-0.629 $\frac{W}{mK}$	1.5×10^{-7} $\frac{m^2}{s}$
2	7-27	69-92							

Table 3: Properties of Tested Ferrofluid.

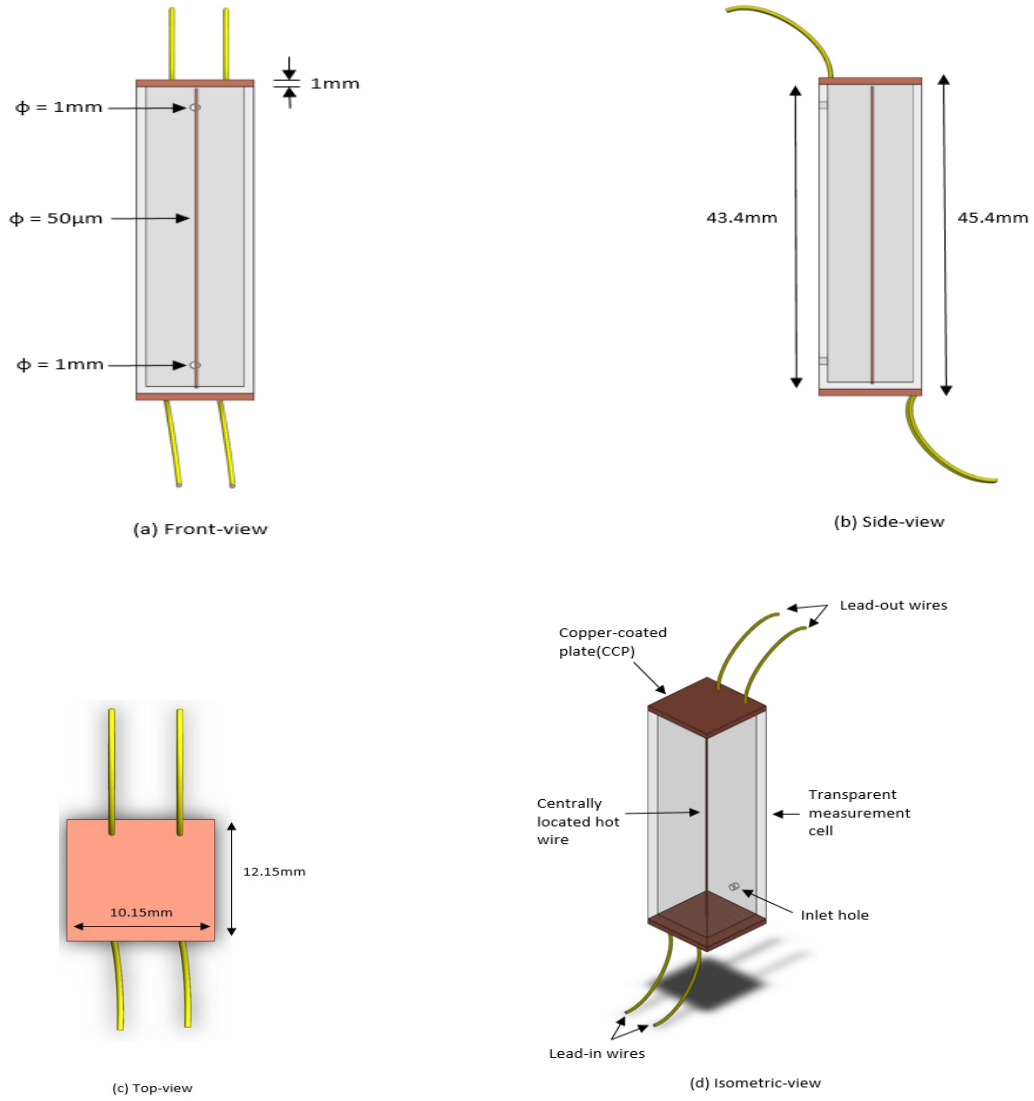

Fig.4: Design and geometry of measurement cell.

The schematic diagram of experimental setup is shown in **Fig.5**. At different constant currents (different power inputs), the voltage drop over the wire is measured by a digital multimeter (Keithley 2700) connected to a personal computer. The induced magnetic field at the surface of the heated micro-wire is 16mT, 14 mT and 12 mT at current supply of 2A, 1.75A and 1.5A. The values are calculated by biot-savarts law of electromagnetism **(Eqn. 6).** Both the electric current source and the voltage recording are triggered automatically using a LABVIEW program. The current supply starts after 0.25 s and the multimeter voltage is recorded after every 0.05 s.

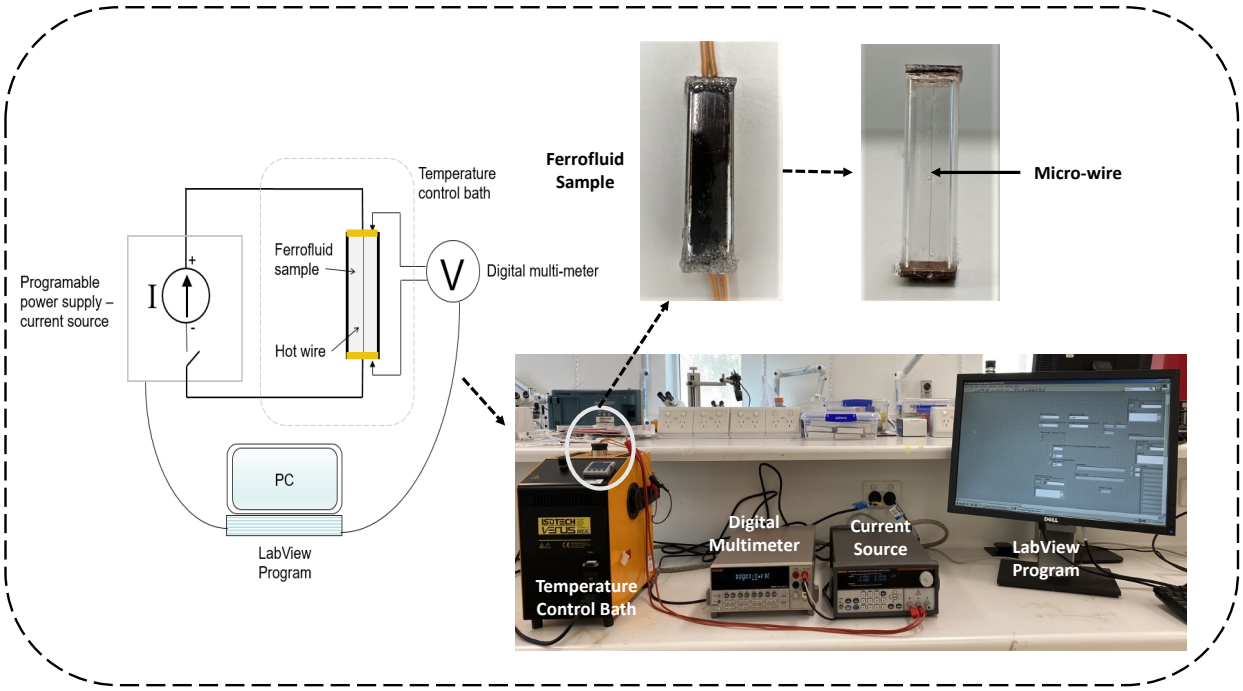

Fig.5: Line Diagram and experimental setup.

The wire resistance is determined via Ohms law and then converted into temperature of the wire using the temperature coefficient of resistance (α) of wires as;

$$\Delta T = \frac{\left(\frac{R}{R_0}-1\right)}{\alpha} \qquad \textbf{(26)}$$

where R_0 is the resistance of the unheated wire. Before calculating the temperature rise, R_0 needs to be determined. This was done by extrapolating the resistance measured from two different currents against the square of the current **[40].** It is not accurate to simply use an Ohm-meter to determine the initial resistance since the measuring current heats the wire and changes the resistance. The measured values of R_0 for the two-copper wire and two platinum wire probes at 20 °C were 0.430 Ω, 0.4293 Ω and 2.6798 Ω., 2.6499 Ω, respectively.

To quantify the heat transfer characteristics of ferrofluid, the average heat transfer coefficient $\bar{h}$ and the Nusselt number $\overline{Nu}$ are calculated by using following relations;

$$\overline{Nu} = \frac{\bar{h}L}{k_{eff}}; \quad \textbf{(27)}$$

where L is the characteristic length (wire length), k_{eff} is the thermal conductivity, (calculated from Eqn. 22) and $\bar{h}$ is the average heat transfer coefficient, defined as

$$\bar{h} = \frac{q_s}{A(T_{wire} - T_0)}; \quad \textbf{(28)}$$

where q_s is surface heat flux generated by Joule heating, A is the surface area of wire and T_{wire} is the temperature of wire.

Table 4: Material Properties for the determination of the Nusselt Number

Symbol	Property	Value
α	Temperature Coefficient copper, platinum	0.004041 °C^{-1}, 0.003729 °C^{-1}
β	Specific resistivity of copper	1.76067×10^{-8} Ω m
c_u	Specific heat of copper	386 J kg^{-1} K^{-1}
c_p	Specific heat of ferro-particles	670 J kg^{-1} K^{-1}
T_0	Initial temperature	293 K
T_{fr}	Freezing Temperature of Water	273 K
ε	Volume Fraction of Suspended particles	0.02
ρ_f	Density of Water	998.2 kg m^{-3}
ρ_p	Density of Suspended particles	5200 kg m^{-3}
k_f	Thermal conductivity of water	0.6 W m^{-1} K^{-1}
k_p	Thermal conductivity of ferroparticle	3 W m^{-1} K^{-1}
d_p	Diameter of suspended particles	10^{-8} m
μ_f	Dynamic Viscosity of Water	1.002×10^{-3} kg m^{-1} s^{-1}

M_f	Molar Mass of water	18.015×10^{-3} kg mol^{-1}

5. Uncertainty Analysis

For reliability of the experimental results, inaccuracies in input variables due to errors in measurement instruments are considered for the estimation of output parameters. The equipment's have the following accuracies: Keithley 2200-20-5 power source 0.05% or 0.1 mA, Keithley 2700 Mustimeter 0.001% or 2mV and Isotech^{TM} controlled bath (T_0) 0.3 °C. The uncertainty in the measured wire temperature is taken as 2%. The corresponding effect of each variable are outlined in **Table 5.** These results are comparable with data reported by Vatani et al.**[17].**

Table 5: Uncertainty Analysis

Variable	**Uncertainty**	q_s=$f(V,I)$	$\overline{Nu}$=$f(\bar{h},L,k)$
Current (A)	<0.05% or 0.1 mA	0.05 %	0.05 %
Voltage (V)	<0.001% or 2mV	0.001%	0.001 %
ΔT	2 %	-	2.15%
Temperature (T_0)	0.3 °C	-	-
L	±1 mm	-	2.29%
k	1%	-	1%
	Combined	**0.05%**	**3.38%**

6. Deviation in Results

Deviations between the results for the model and experiment may be attributed to geometrical imperfections and secondary thermomagnetic fluid phenomena. First, measurement cell as well as the wire are perfectly aligned with the gravity vector in the simulations, possible deviations occur in the experiments. Second, the simulation does not account the wire's volumetric expansion with temperature, leading to deviation from the perfectly central position, resulting in non-axisymmetric temperature fields. Moreover, differences between theory and experiment show that there is room for further improvement of the ferrofluid model. For instance, magnetoviscous effects [48] have been neglected which would tend to suppress thermomagnetic convection and could help explain why predicted temperatures in Figs are lower than the measured values. The model also neglects phenomena such as magnetophoresis

and thermophoresis. It is conceivable that these phenomena will have greater influence at larger values of time causing model departures from the measurements at large time.

7. Results and Discussion

The observed transient behaviour of the temperature curves for a heated micro-wire immersed in fluids can be explained through a combination of heat conduction, natural convection and thermomagnetic convection. The inception of natural and thermomagnetic convection in fluid can be recognized on the graph of temperature against time as a divergence in the linearity of the curve **[17].** This section shows clear evidence that the strength of the axisymmetric magnetic field has a significant effect on cooling.

7.1 Experimental Results

The effect of the self-induced magnetic field can be found through comparing the temperature rise in ferrofluid and DIW when different currents are supplied to copper and platinum microwires to achieve the same Joule heating. **Fig. 6** shows the results of the experiment. The experiments were conducted with a constant initial and boundary temperature of 293.15 K and three different current values of 1.5 A, 1.75 A, 2 A and 0.615 A, 0.7175 A, 0.82 A are being supplied to the copper and platinum cells respectively for 12 s to acquire the same joule heating of 1.005 W, 1.384 W and 1.834 W respectively. Measurements at 0.438 W and 0.689 W are also done as shown in **Fig. 6** but the phenomenon under investigation is less clear than at the higher electrical powers.

The measured temperature rises of the heated wire against time shown in **Fig. 6** give good insight into the heat transfer characteristics of the fluid. A lower temperature rise for the same power means better heat transfer. If we consider the case of 1.834 W in **Fig. 6** we can see that initially (up until $\log(t) \approx -0.4$) all of the curves coincide with each other. In this initial region the dominant mechanism for heat transfer is heat conduction. This phenomenon of initial heat conduction domination is used to measure thermal conductivity of fluids in the transient hot-wire method **[41].** If we consider the measurements taken in DIW, the conduction-dominated region continues for a time period of the order of one or two seconds and then natural convection becomes the dominant mechanism for heat transfer. This causes a local maximum in the curve at around $\log(t) \approx 0.35$ in **Fig. 6** for 1.834 W in DIW. The subsequent decrease/drop

in temperature results from the natural convection intensifying the heat transfer between wire and fluid **[42].**

The agreement between the curves for platinum and copper in DIW in **Fig. 6** confirms that the self-induced magnetic field does not affect the natural convection phenomenon. Moreover, the consistent temperature rise of Pt and Cu wires in DIW at the same Joule heating shows that differences in heat conduction out the ends of the wires (due to different metal thermal conductivities) are not greatly affecting the results.

The lower temperatures for the wires in ferrofluid in **Fig. 6** show the enhanced heat transfer due to thermomagnetic convection. Variation in the self-induced magnetic field strength has remarkable effect on heat transfer by ferrofluid as can be seen by comparing the temperature change for platinum and copper wires (e.g. 'Pt with FF' and 'Cu with FF' at 1.834 W in **Fig. 6).** The higher electrical current in the case of copper causes a very early departure from the conduction heat transfer dominated regime ($\log(t) \approx -0.35$). The platinum wire in ferrofluid, on the other hand behaves the same as the DIW case until about $t \approx 1$ second. This suggests that thermomagnetic convection effects become stronger for the larger electric current earlier due to the stronger self-induced magnetic field.

By using the two different conductor materials, **Fig. 6** provides the strongest experimental evidence to date from our group that thermomagnetic convection can occur for a single conductor due only to the magnetic field produced by the current in the wire itself. The enhanced cooling effect is certainly due to the magnetic field interacting with the magnetic particles. On comparing the temperature change between copper and platinum wires, the cooling effect is much stronger in copper micro-wire at the same Joule heating. For 1.834 W Joule heating, the temperature of the copper wire is 6 K lower than that of the platinum wire ($\log(t) \approx$ 0.2s to 0.6s). This analysis experimentally proves the effect of the self-induced magnetic field on the thermomagnetic cooling effect of ferrofluids on a microwire without an externally applied magnetic field.

For large time ($\log(t) > 0.8$) in **Fig. 6**, an unexpected phenomenon can be observed where the temperature of the copper wire in the ferrofluid becomes greater than that of the platinum wire (most clearly seen for 1.834 W). This may be due to the beginnings of separation of the

magnetic nanoparticles from the fluid and accumulation on the wire. A careful examination of the wire after the experiments showed some darkening of the wire surface. Other possible explanations include magnetophoresis causing an increased viscosity or thermophoresis driving particle movement relative to the base fluid.

A further observation from **Fig. 6** is that the thermomagnetic convection phenomenon is clearest for the highest electrical power cases. This makes sense since a higher electrical current is needed to make a stronger magnetic field. Moreover, the temperature gradients needed to produce the changes in magnetic susceptibility are greater for higher heating powers.

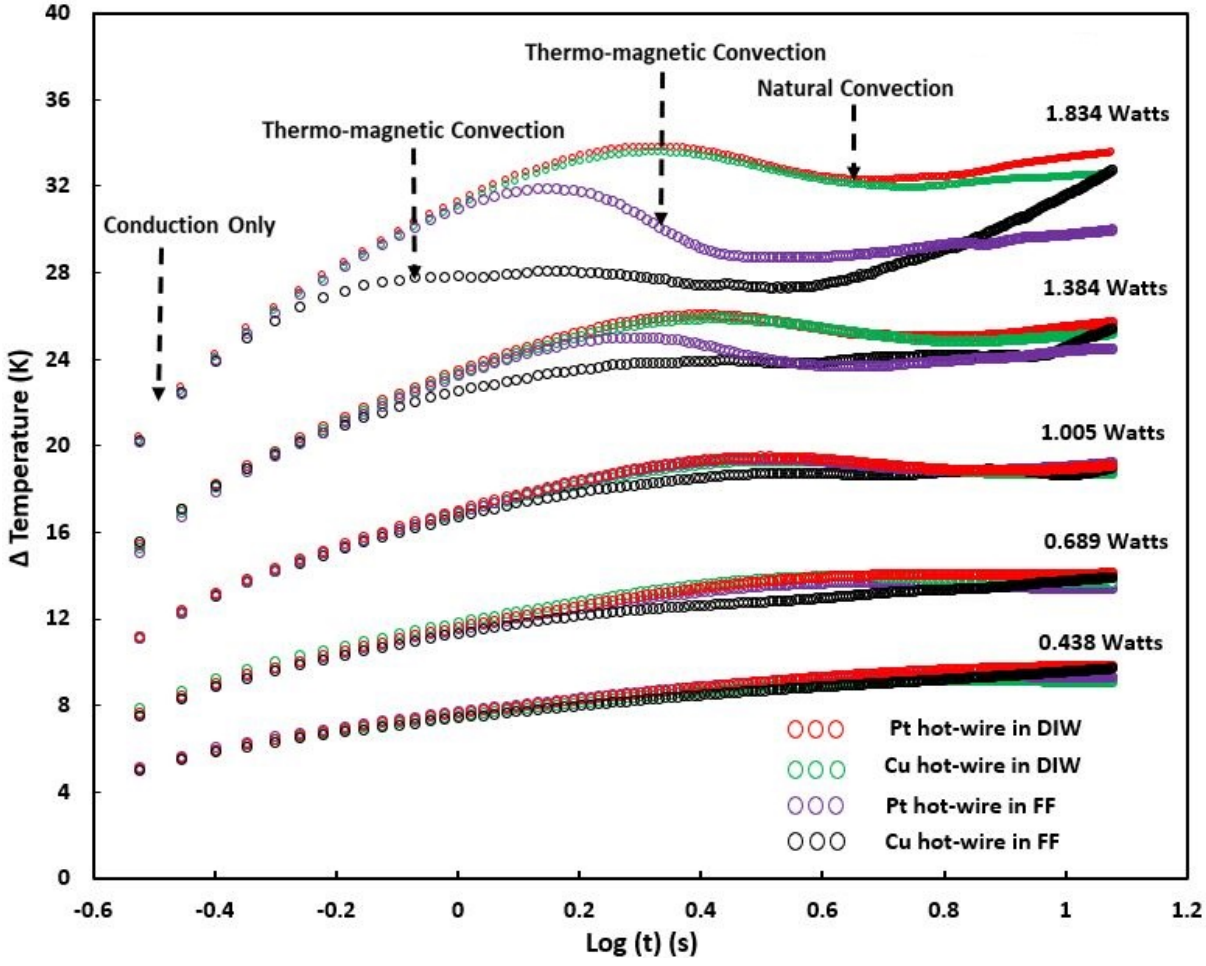

Fig.6: Experimental results.

7.2 Comparison of Simulation and Experiment

Fig.7 presents the temperature rise in the copper wire surrounded by DIW at current supplies of 1.5A and 2A for 12 seconds to the measurement cell showing both simulation and experimental results. This example is only concerned with natural convection since the fluid is water. Both experiment and simulation show the same trend with an initial conduction-dominated regime followed by a cooler, steadier behaviour. In the case of 2 A at large time,

the predicted cooling effect is less significant than that observed in the experiment. Overall, there is a reasonable agreement between theory and experiment for the natural convection simulation.

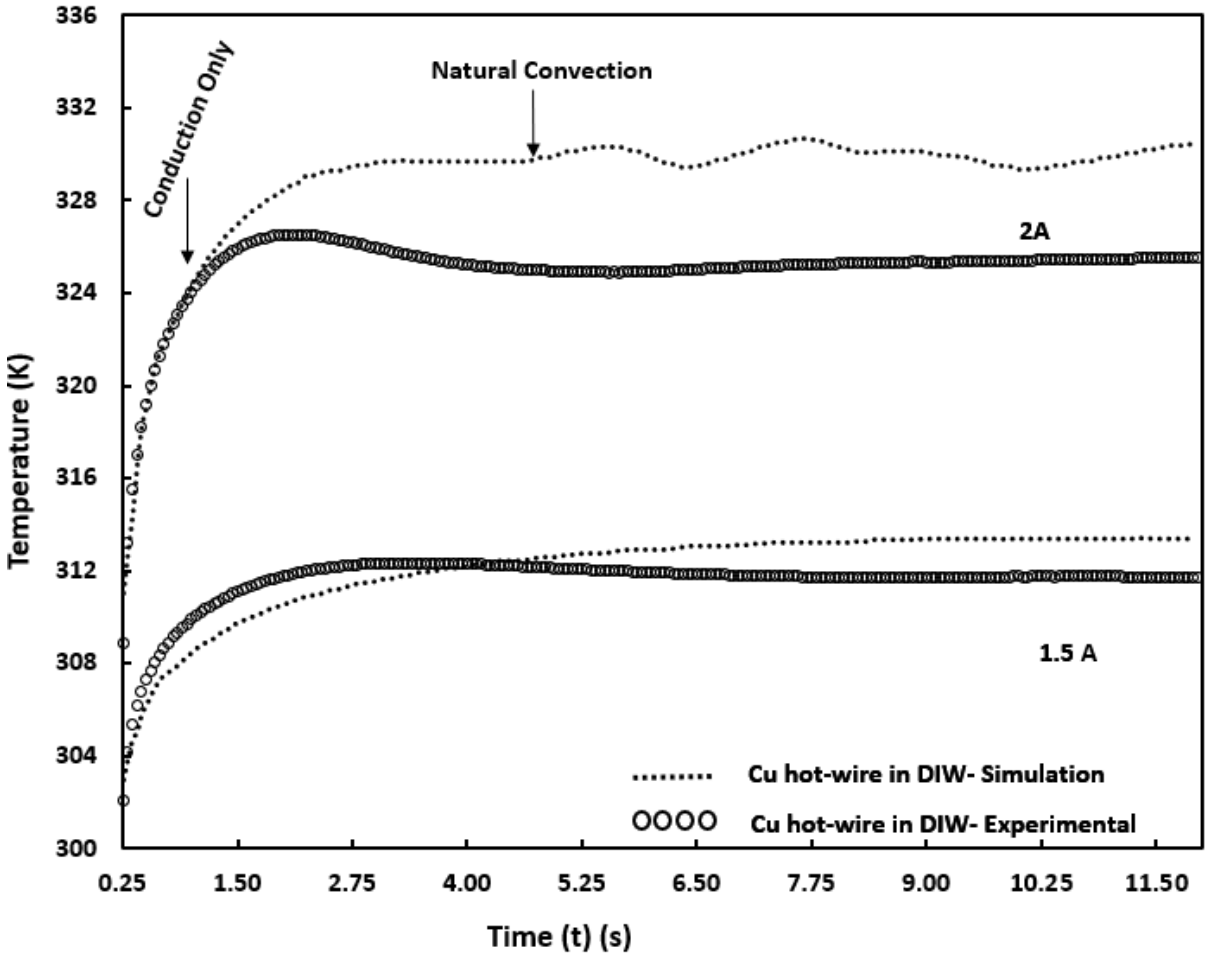

Fig. 7: Cu Wire Temperature at different Currents in DIW

From fig. 7, at significant time points, the temperature and velocity contours at 2A current supply are presented in **fig. 8** and **fig. 9**. With time, rise in temperature of wire is causing the increase in flow field velocity and more heat is transported from the heated wire. Heat is flowing with the convection field upwards towards the cell's upper end. As the temperature increment is the reason for buoyancy driven flow, further heating causes a stronger connective flow, cooling down the wire again. With time, fluid becomes warmer and starts flowing upwards. Hence the fluid around the wire on the upper side does not cool down the wire in the same amount as fluid on the bottom. The fluid's increasing temperature along the wire length also cause the flow field to accelerate along the length and finally flow field's velocity increases which is shown in the **fig. 9**.

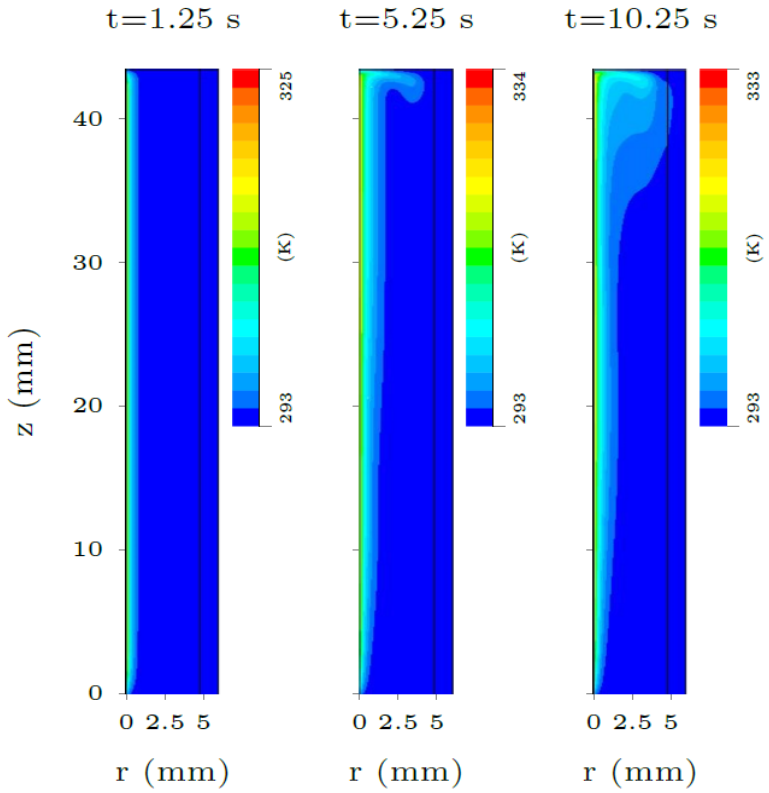

Fig.8: Temperature contour plots (K) from simulation for DIW with copper wire and 2 A

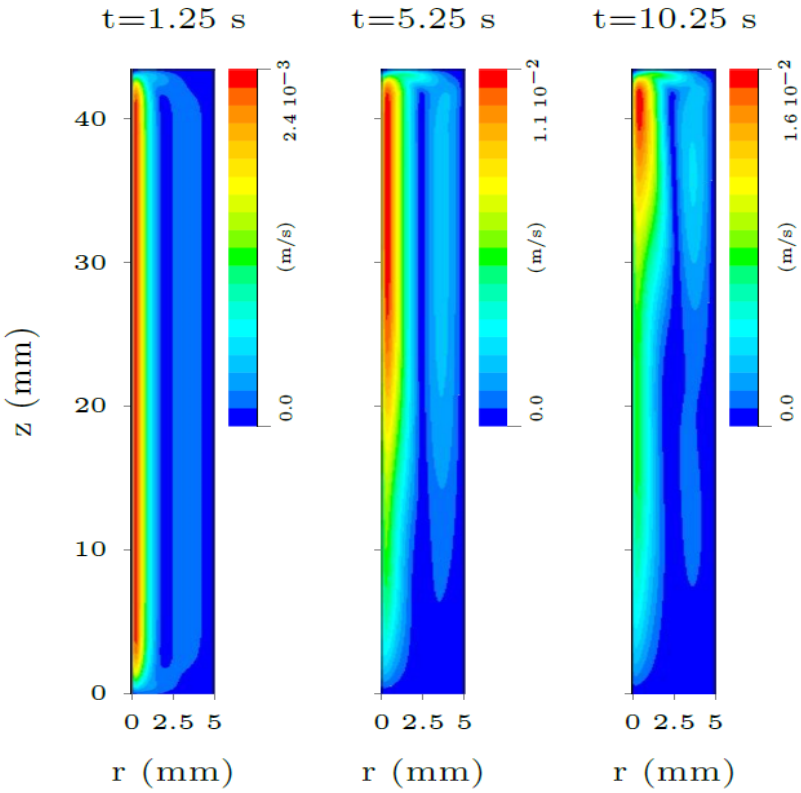

Fig.9: Velocity contour plots (m/s) from simulation for DIW with copper wire and 2 A

Fig. 10 compares simulations and experiment for the case of a copper wire in ferrofluid where thermomagnetic convection super-imposes natural convection. The agreement is at a similar

level to that of the natural convection prediction in **Fig. 7**. Generally, the predictions shown in **Fig. 10** suggest a greater cooling effect due to thermomagnetic convection than that observed in the experiment. Nevertheless, in both cases, due to combined natural and thermomagnetic convection in later phase, the temperature of the wire drops significantly. These results suggest that the present model overpredicts the cooling effect but captures the phenomenon.

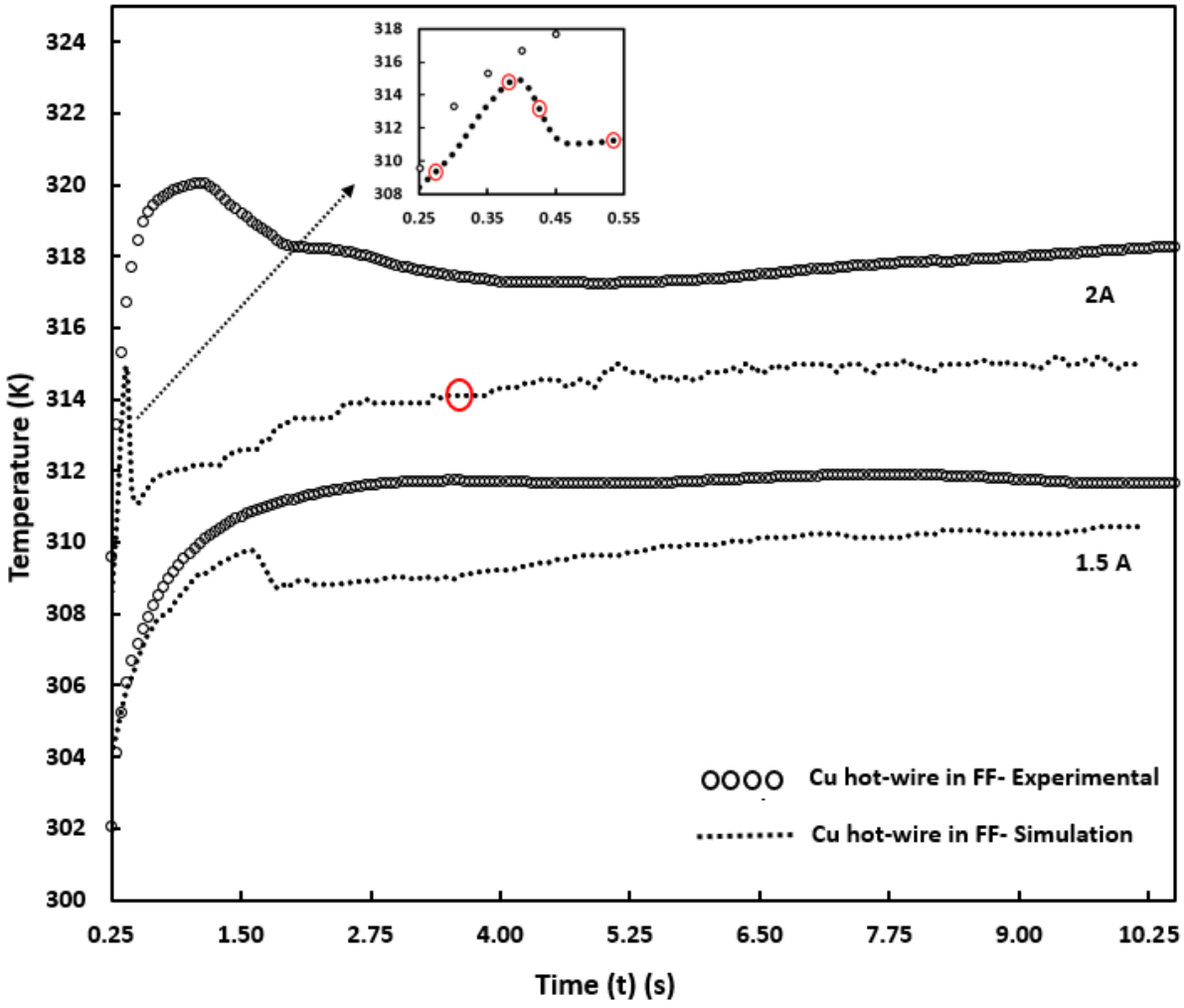

Fig.10: Cu Wire Temperature at different currents in ferrofluid

In **Fig.11** the ferrofluid's Nusselt number's slope is smaller, meaning that the heat flux across the wire surface decreases slower in ferrofluid case and therefore more heat is conducted into the ferrofluid for a longer period due to better heat transfer capacity of the ferrofluid. Moreover, a higher Nusselt number appears for higher temperature gradients. Due to Nusselt number's relation to the temperature difference ($Nu \propto h \propto T^{-1}$), even a small drop in temperature can cause high change in Nusselt Numbers. Since the Nusselt number for ferrofluid case is higher, at faster rate heat is transported away from the wire's surface and occurs due to thermomagnetic convection in addition to natural convection.

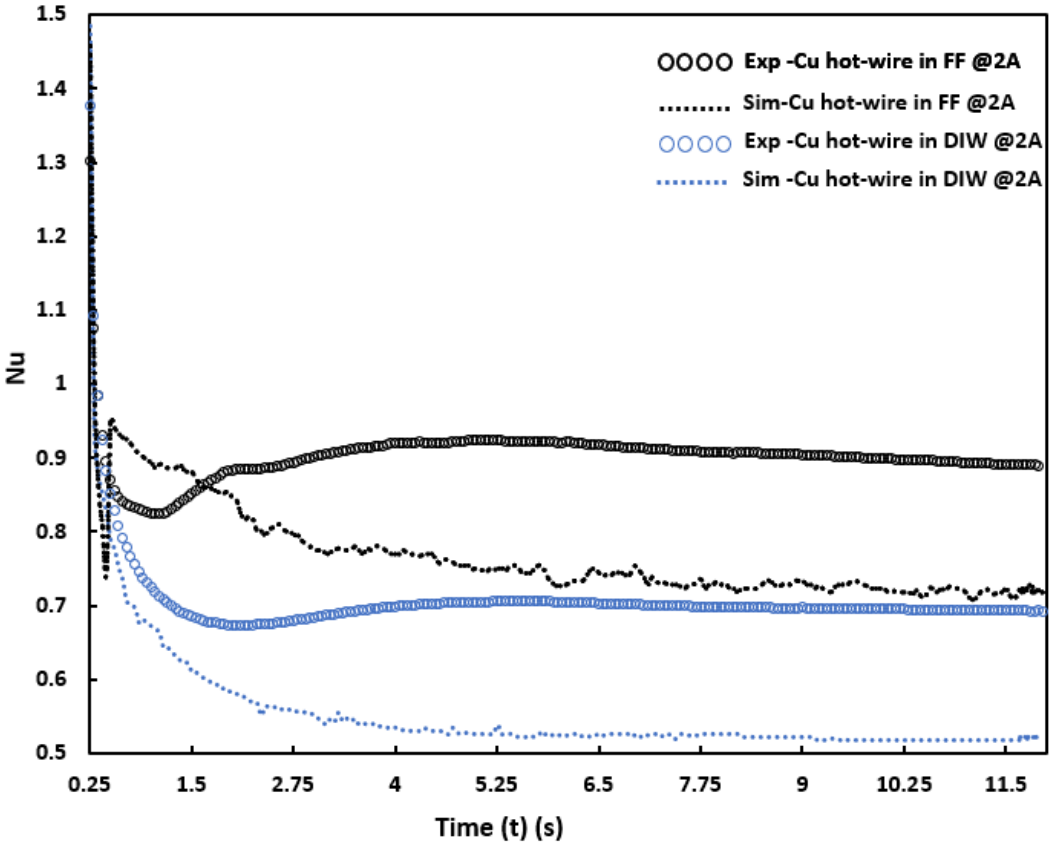

Fig.11: Variation in Nusselt Number with copper wire and 2 A

7.3 Thermomagnetic Convection Cells

One of the issues with experimental studies on ferrofluids is that the dark colour of the suspension makes it difficult to visualize thermomagnetic convection effects. Numerical simulations have no such limitation. Since the model considered here is broad enough to capture natural convection and thermo-magnetic convection it is interesting to examine the development of the thermal field during heating of the wire.

Fig. 12 shows simulation results for the thermal field at significant time points. At time t = 0.26 s only a thin layer of ferrofluid is heating up and heat transfer is dominated by steady state conduction. Initial effects caused by the thermomagnetic convection can be considered at the next point where t = 0.385 s. At this position, the temperature distribution is unsteady and flow recirculation sets-in with time. Cold fluid with a stronger magnetic body force flows towards the heated wire, becomes warm again and then experiences a relative body force away from the wire. This recirculation transports the thermal energy gained previously away from wire having a local cooling effect on the wire and causing the thermo-magnetic vortices near the wire surface. These thermomagnetic convection cells become larger as time progresses.

In addition to the axial velocities associated with natural convection, radial velocities due to the temperature dependence of magnetic susceptibility, appearing as thermomagnetic body forces perpendicular to the wire. Positive, as well as negative radial velocities can be identified in **Fig.13.** As warmer fluid is pushed away by the magnetic pressure close to the wire, it becomes colder again, due to the temperatures being colder at greater distances from the wire. Hence the cold fluid increases again in magnetic susceptibility, causing a stronger body force, pulling the cold fluid back to the wire. Because of such recirculation around the wire surface, there is a continuous fluctuation in the absolute temperature of wire and Nusselt number; correspondingly simulation curves are wavy.

Since the temperature field has a steeper gradient in radial direction, the thermomagnetic convection occurs in a smaller geometric scale. Further from the wire, temperature gradients are not sufficiently high to cause variations in the magnetic body force. In addition to this, the Nusselt number which is proportional to the heat flux on the wire's surface and temperature gradient, are higher for this region.

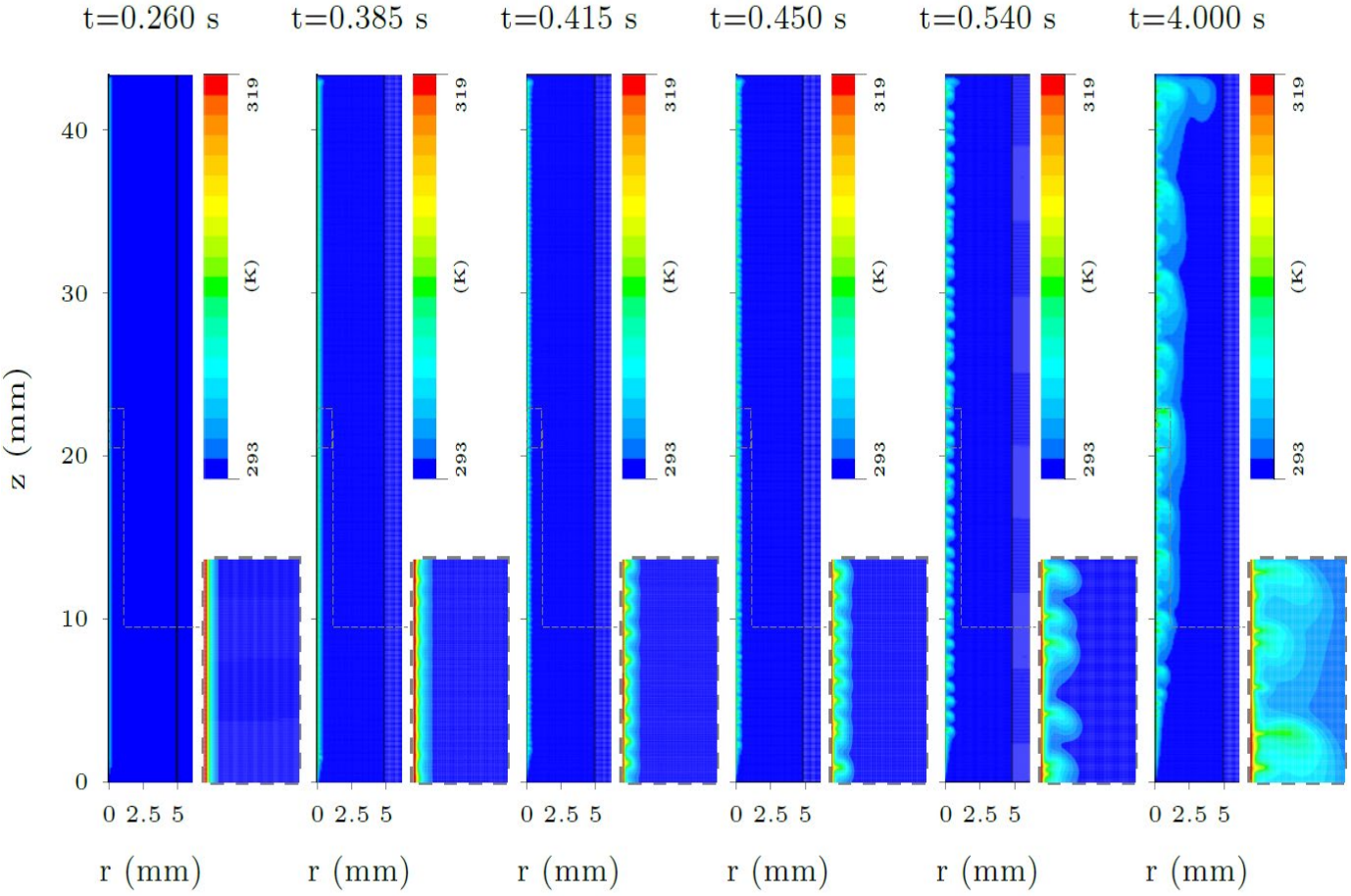

Fig.12: Temperature contour plots (K) from simulation for ferrofluid with copper wire and 2 A

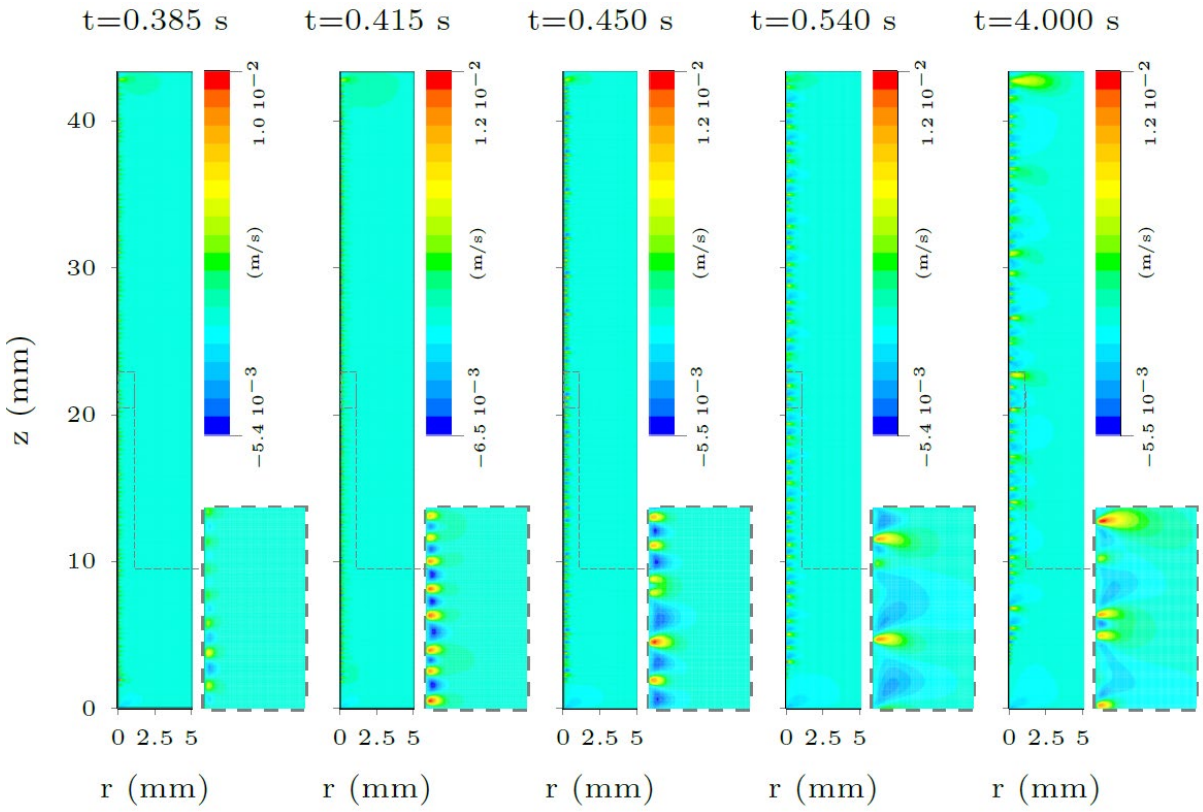

Fig.13: Velocity contour plots (m/s) from simulation for ferrofluid with copper wire and 2 A

8. Conclusion

Thermomagnetic convection by ferrofluid around electrically heated micro-wires in a square channel is observed experimentally and simulated numerically. Results are compared with natural convection in DIW under the same operational conditions. Flow and heat transfer characteristics during thermomagnetic convection at ideal conditions are simulated and presented at significant timings. For the same Joule heating, the effect of the wire's self-induced magnetic field on thermomagnetic convection is determined and consequently a drop in temperatures is observed. The major outcomes are summarized as;

- The observed heat transfer enhancement by ferrofluid is due to thermomagnetic convection instead of enhanced natural convection due to modified effective properties.
- Thermomagnetic convection superimposes the natural convection in ferrofluids, and a higher temperature drop is observed. This phenomenon dominates at higher current supply.
- Stronger self-induced magnetic fields around the copper wire compared with the platinum wire resulted in higher cooling effects by thermomagnetic convection. Conductor material is a critical parameter for thermomagnetic convection.

- Agglomeration of ferro-particles resulted into degraded heat transfer for large time.
- More cooling effect around the bottom of wire by DIW, consequently flow field's velocity increases along the wire length.
- Flow recirculation generates thermal vortices in ferrofluid that result in local cooling along the wire vicinity due to variation of magnetic susceptibility with temperature.

Conflict of Interest

None

Acknowledgments

The corresponding author is thankful to Higher Degree Research scholarships from Griffith University.

References

[1] Bahiraei M, Hangi M. Flow and heat transfer characteristics of magnetic nanofluids: a review. J. Magn. Magn. Mater. 2015; 374: 125-138. https://doi.org/10.1016/j.jmmm.2014.08.004

[2] Gui NGJ, Stanley C, Nguyen NT, Rosengarten G. Ferrofluids for heat transfer enhancement under an external magnetic field. Int. J. Heat Mass Transf. 2018;123: 110-121. https://doi.org/10.1016/j.ijheatmasstransfer.2018.02.100

[3] Nkurikiyimfura I, Wang Y, Pan Z. Heat transfer enhancement by magnetic nanofluids—a review. Renew. Sust. Energ. Rev.2013; 21:548-561. https://doi.org/10.1016/j.rser.2012.12.039

[4] Wu S, Ortiz CR. Experimental investigation of the effect of magnetic field on vapour absorption with LiBr–H_2O nanofluid. Energy.2020;193:116640. https://doi.org/10.1016/j.energy.2019.116640

[5] Sheikholeslami M, Ganji, DD. Ferrohydrodynamic and magnetohydrodynamic effects on ferrofluid flow and convective heat transfer. Energy.2014;75:400-410. https://doi.org/10.1016/j.energy.2014.07.089

[6] Fornalik-Wajs E, Roszko A, Donizak J. Nanofluid flow driven by thermal and magnetic forces–Experimental and numerical studies. Energy 2020;201:117658. https://doi.org/10.1016/j.energy.2020.117658

[7] Solangi KH, Kazi SN, Luhur MR, Badarudin A, Amiri A, Sadri R, Zubir MNM, Gharehkhani S, Teng KH. A comprehensive review of thermo-physical properties and convective heat transfer to nanofluids. Energy 2015;89:1065-1086.

https://doi.org/10.1016/j.energy.2015.06.105

[8] Vatani A,Woodfield PL, Nguyen NT, Dao DV. Thermomagnetic convection around a current-carrying wire in ferrofluid. J. Heat Transfer 2017;139:104502. https://doi.org/10.1115/1.4036688

[9] Krakov MS, Nikiforov IV. Influence of the shape of the inner boundary on thermomagnetic convection in the annulus between horizontal cylinders: Heat transfer enhancement. Int. J. Therm. Sci.2020; 153:106374. https://doi.org/10.1016/j.ijthermalsci.2020.106374

[10] Engler H, Lange A, Borin D, Odenbach S. Hindrance of thermomagnetic convection by the magnetoviscous effect. Int. J. Heat Mass Transf.2013: 60: 499-504. https://doi.org/10.1016/j.ijheatmasstransfer.2012.10.049

[11] Shuchi S, Sakatani K, Yamaguchi H. An application of a binary mixture of magnetic fluid for heat transport devices. J. Magn. Magn. Mater. 2015; 289:257-259. https://doi.org/10.1016/j.jmmm.2004.11.073.

[12] Goharkhah M, Ashjaee M, Shahabadi M.Experimental investigation on convective heat transfer and hydrodynamic characteristics of magnetite nanofluid under the influence of an alternating magnetic field. Int. J. Therm. Sci. 2016;99:113-124. https://doi.org/10.1016/j.ijthermalsci.2015.08.008

[13] Mehrali M, Sadeghinezhad E, Akhiani AR, Latibari ST, Metselaar HSC, Kherbeet AS, Mehrali M. Heat transfer and entropy generation analysis of hybrid graphene/Fe_3O_4 ferro-nanofluid flow under the influence of a magnetic field. Powder Technol.2017;308:149-157. https://doi.org/10.1016/j.powtec.2016.12.024

[14] Vatani A, Woodfield PL, Dinh T, Phan HP, Nguyen NT, Dao DV. Degraded boiling heat transfer from hotwire in ferrofluid due to particle deposition. Appl. Therm. Eng. 2018;142:255-261. https://doi.org/10.1016/j.applthermaleng.2018.06.064

[15] Xuan Y, Lian W. Electronic cooling using an automatic energy transport device based on thermomagnetic effect. Appl. Therm. Eng.2011;31:1487-1494. https://doi.org/10.1016/j.applthermaleng.2011.01.033

[16] Krauzina MT, Bozhko AA, Krauzin PV, Suslov SA. The use of ferrofluids for heat removal: Advantage or disadvantage? J. Magn. Magn. Mater. 2017; 431:241-244. https://doi.org/10.1016/j.jmmm.2016.08.085

[17] Vatani A, Woodfield PL, Nguyen NT, Dao DV. Onset of thermomagnetic convection around a vertically oriented hot-wire in ferrofluid. J. Magn. Magn. Mater. 2018;456:300-306. https://doi.org/10.1016/j.jmmm.2018.02.040

[18] Wen CY, Su WP. Natural convection of magnetic fluid in a rectangular Hele-Shaw cell. J. Magn. Magn. Mater. 2005;289, 299-302. https://doi.org/10.1016/j.jmmm.2004.11.085

[19] Zablotsky D, Mezulis A, Blums E. Surface cooling based on the thermomagnetic convection: Numerical simulation and experiment. Int. J. Heat Mass Transf. 2009;52:5302-5308. https://doi.org/10.1016/j.ijheatmasstransfer.2009.08.001

[20] Lajvardi M, Moghimi-Rad J, Hadi I, Gavili A, Isfahani TD, Zabihi F, Sabbaghzadeh J. Experimental investigation for enhanced ferrofluid heat transfer under magnetic field effect. J. Magn. Magn. Mater. 2010; 322:3508-3513. https://doi.org/10.1016/j.jmmm.2010.06.054

[21] Jin L, Zhang X, Niu X. Lattice Boltzmann simulation for temperature-sensitive magnetic fluids in a porous square cavity. J. Magn. Magn. Mater. 2015;324:44-51. https://doi.org/10.1016/j.jmmm.2011.07.033

[22] Mukhopadhyay A, Ganguly R, Sen S, Puri, IK. A scaling analysis to characterize thermomagnetic convection. Int. J. Heat Mass Transf. 2005;48:3485-3492. https://doi.org/10.1016/j.ijheatmasstransfer.2005.03.021

[23] Jafari A, Tynjälä T, Mousavi SM, Sarkomaa P. Simulation of heat transfer in a ferrofluid using computational fluid dynamics technique. Int. J. Heat Fluid Flow.2008; 29:1197-1202. https://doi.org/10.1016/j.ijheatfluidflow.2008.01.007

[24] Ashouri M, Ebrahimi B, Shafii MB, Saidi MH, Saidi MS. Correlation for Nusselt number in pure magnetic convection ferrofluid flow in a square cavity by a numerical investigation. J. Magn. Magn. Mater. 2010;322:3607-3613. https://doi.org/10.1016/j.jmmm.2010.05.041

[25] Strek T, Jopek H. Computer simulation of heat transfer through a ferrofluid. Physica status solidi. 2007;244:1027-1037. https://doi.org/10.1002/pssb.200572720

[26] Bahiraei M, Hangi M, Rahbari A. A two-phase simulation of convective heat transfer characteristics of water–Fe_3O_4 ferrofluid in a square channel under the effect of permanent magnet. Appl. Therm. Eng.2019;147:991-997. https://doi.org/10.1016/j.applthermaleng.2018.11.011

[27] Hangi M, Bahiraei M, Rahbari A. Forced convection of a temperature-sensitive ferrofluid in presence of magnetic field of electrical current-carrying wire: A two-phase approach. Adv. Powder Technol. 2018, 29; 2168-2175. https://doi.org/10.1016/j.apt.2018.05.026

[28] Vatani A, Woodfield PL, Nguyen NT, Abdollahi A, Dao DV. Numerical simulation of combined natural and thermomagnetic convection around a current carrying wire in ferrofluid. J. Magn. Magn. Mater. 2019;489:165383. https://doi.org/10.1016/j.jmmm.2019.165383

[29] Cunha LH, Siqueira IR, Campos AA, Rosa AP, Oliveira TF. A numerical study on heat transfer of a ferrofluid flow in a square cavity under simultaneous gravitational and magnetic convection. Theor. Comput. Fluid Dyn.2020;34:119–132. https://doi.org/10.1007/s00162-020-00515-1

[30] Szabo PS, Früh WG. The transition from natural convection to thermomagnetic convection of a magnetic fluid in a non-uniform magnetic field. J. Magn. Magn. Mater. 2018; 447:116-123. https://doi.org/10.1016/j.jmmm.2017.09.028

[31] Singh D, Shyam S, Mehta B, Asfer M, Alshqirate AS.Exploring Heat Transfer Characteristics of Ferrofluid in the Presence of Magnetic Field for Cooling of Solar Photovoltaic Systems. J. Thermal Sci. Eng. Appl 2019; 11(4): 041017. https://doi.org/10.1115/1.4044188

[32] Dalvi S, Karaliolios ECJ, van der Meer TH, Shahi M. Thermo-magnetic convection in a circular annulus filled with magnetocaloric nanofluid. Int. Commun. Heat Mass.2020; 116:104654. https://doi.org/10.1016/j.icheatmasstransfer.2020.104654

[33] Gerdroodbary MB, Sheikholeslami M, Mousavi SV, Anazadehsayed A and Moradi R. 2018. The influence of non-uniform magnetic field on heat transfer intensification of ferrofluid inside a T-junction. Chem. Eng. Process.2018;123:58-66. https://doi.org/10.1016/j.cep.2017.10.021

[34] Sheikholeslami M and Rashidi MM. 2015. Ferrofluid heat transfer treatment in the presence of variable magnetic field. Eur. Phys. J. Plus. 2015;130:115-127.

https://doi.org/10.1140/epjp/i2015-15115-4

[35] Sheikholeslami M, Nimafar M and Ganji DD. Nanofluid heat transfer between two pipes considering Brownian motion using AGM. Alexandria engineering journal.2017;56: 277-283. https://doi.org/10.1016/j.aej.2017.01.032

[36] Sheikholeslami M, Ganji DD, Javed MY and Ellahi R. 2015. Effect of thermal radiation on magnetohydrodynamics nanofluid flow and heat transfer by means of two-phase model. J. Magn. Magn. Mater.2015;374:36-43. https://doi.org/10.1016/j.jmmm.2014.08.021

[37] Shafee A, Shahraki MS, Taleghani AH, Nam ND and Tlili I. Analysis of nanomaterial flow among two circular tubes in the presence of magnetic force. J. Therm. Anal. Calorim. 2020:1-10. https://doi.org/10.1007/s10973-020-09555-5

[38] Odenbach S. Microgravity experiments on thermomagnetic convection in magnetic fluids. J. Magn. Magn. Mater.1995;149:155-157. https://doi.org/10.1016/0304-8853(95)00360-6

[39] Corcione M. Empirical correlating equations for predicting the effective thermal conductivity and dynamic viscosity of nanofluids. Energy Convers. Manag. 2011;52:789-793. https://doi.org/10.1016/j.enconman.2010.06.072

[40] Woodfield PL, Moroe S, Fukai J, Fujii M, Shinzato K, Kohno M, Takata Y. Techniques for accurate resistance measurement in the transient short-hot-wire method applied to high thermal-diffusivity gas. Int. J. Thermophys. 2009;30:1748. https://doi.org/10.1007/s10765-009-0668-1

[41] Moroe S, Woodfield PL, Kimura K, Kohno M, Fukai J, Fujii, M, Shinzato K, Takata Y. Measurements of hydrogen thermal conductivity at high pressure and high temperature. Int. J. Thermophys.2011;32:1887. https://doi.org/10.1007/s10765-011-1052-5

[42] Nagasaka Y, Nagashima A. Simultaneous measurement of the thermal conductivity and the thermal diffusivity of liquids by the transient hot-wire method. Rev. Sci. Instrum.1981;52:229-232. https://doi.org/10.1063/1.1136577

[43] Ghasemian M, Ashrafi ZN, Goharkhah M, Ashjaee M. Heat transfer characteristics of Fe_3O_4 ferrofluid flowing in a mini channel under constant and alternating magnetic fields. J. Magn. Magn. Mater.2015;381:158-167. https://doi.org/10.1016/j.jmmm.2014.12.078

[44] Lange A. Kelvin force in a layer of magnetic fluid. J. Magn. Magn. Mater.2002; 241:327-329. https://doi.org/10.1016/S0304-8853(01)01368-3

[45] Rahman H, Suslov SA. Thermomagnetic convection in a layer of ferrofluid placed in a uniform oblique external magnetic field. J. Fluid Mech.2015;764:316. https://doi.org/10.1017/jfm.2014.709

[46] Buongiorno J. Convective transport in nanofluids. J. Heat Transfer. 2006; 28:240-250 https://doi.org/10.1115/1.2150834

[47] Kraszewska A, Pyrda L and Donizak J. High magnetic field impact on the natural convection behaviour of a magnetic fluid. 2018 Heat Mass Transf. 2018; 54:2383-2394. https://doi.org/10.1007/s00231-017-2153-x

[48] Afifah AN, Syahrullail S, and Sidik, NAC. 2016. Magnetoviscous effect and thermomagnetic convection of magnetic fluid: A review. Renew. Sust. Energ. Rev. 2016; 55:1030-1040. https://doi.org/10.1016/j.rser.2015.11.018

Highlights

- Consistent experiments to observe the thermomagnetic convection by ferrofluids.
- Magnetic field effect on thermomagnetic convection under same heat flux boundary conditions.
- Development and validation of 2D model for flow visualization and thermal fields.
- Effects of change in magnetic susceptibility.